Pathogen-specific TLR2 Protein Activation Programs Macrophages to Induce Wnt-β-Catenin Signaling*[S]

Kushagra Bansal[‡1,2], Jamma Trinath[‡1,3], Dipshikha Chakravortty[‡], Shripad A. Patil[§], and Kithiganahalli Narayanaswamy Balaji[‡4]

From the ‡Department of Microbiology and Cell Biology, Indian Institute of Science, Bangalore 560012 and the §Department of Microbiology, National Institute of Mental Health and Neurosciences, 560029 Bangalore, India

Innate immunity recognizes and resists various pathogens; however, the mechanisms regulating pathogen *versus* non-pathogen discrimination are still imprecisely understood. Here, we demonstrate that pathogen-specific activation of TLR2 upon infection with *Mycobacterium bovis* BCG, in comparison with other pathogenic microbes, including *Salmonella typhimurium* and *Staphylococcus aureus*, programs macrophages for robust up-regulation of signaling cohorts of Wnt-β-catenin signaling. Signaling perturbations or genetic approaches suggest that infection-mediated stimulation of Wnt-β-catenin is vital for activation of Notch1 signaling. Interestingly, inducible NOS (iNOS) activity is pivotal for TLR2-mediated activation of Wnt-β-catenin signaling as $iNOS^{-/-}$ mice demonstrated compromised ability to trigger activation of Wnt-β-catenin signaling as well as Notch1-mediated cellular responses. Intriguingly, TLR2-driven integration of iNOS/NO, Wnt-β-catenin, and Notch1 signaling contributes to its capacity to regulate the battery of genes associated with T_{Reg} cell lineage commitment. These findings reveal a role for differential stimulation of TLR2 in deciding the strength of Wnt-β-catenin signaling, which together with signals from Notch1 contributes toward the modulation of a defined set of effector functions in macrophages and thus establishes a conceptual framework for the development of novel therapeutics.

Macrophages as important sentinels of the innate immunity utilize a limited number of pattern recognition receptors, including TLR2 to discriminate among various microbial pathogens and also to mount immune responses commensurate with each pathogen (1, 2). However, the immune cells cannot exclusively utilize "pattern recognition" as the basis of pathogen-specific defense, because a plethora of microbial pathogens share the molecules involved in such recognition with innocuous commensal flora (3, 4). In this regard, macrophages must be able to distinguish the nature and scope of microbial threats to tailor specific transcriptional responses. In this perspective, intensive interplay between signaling pathways can act as an important regulatory mechanism by which the immune responses are tailored against the type of pathogen encountered. However, information about the signaling cascades regulating pathogen-specific TLR2 responses is still imprecisely understood. Interestingly, TLR2 triggering in contrast to current doctrine could lead to tolerogenic or regulatory responses thus conjecturing a role for pathogen-specific activation of TLR2 in immune evasion mechanisms (5–7). Thus, pathogen-specific TLR2-mediated signaling pathways could contribute to unique tailor-made defense responses to invading pathogens. Among signaling events, Wnt-β-catenin signaling plays a critical role in regulation of various cellular processes, including cell polarity, motility, differentiation, apoptosis, and carcinogenesis in both nonvertebrates and vertebrates (8, 9). Wnt ligands secreted from various cell types typically bind to transmembrane receptors of the Frizzled family. This results in activation of multifaceted signaling cascade culminating in marked inhibition of a negative regulator of β-catenin protein levels, glycogen synthase kinase-3β (GSK-3β). The inhibition of GSK-3β leads to nuclear translocation of β-catenin and subsequent activation of lymphoid enhancer factor/T cell factor (LEF1/TCF)[5] target genes (8, 10, 11). Despite reported effects of Wnt signaling on various cell fate decisions, the participation of other vital signaling events involved in defining the inflammatory signatures during ensuing immunity remains to be identified. In this regard, involvement of Notch signaling in conferring specific phenotypical attributes to macrophages and dendritic cells assumes critical importance. Notch signaling is generally initiated by binding of Jagged or Delta, specific ligands of Notch receptor. Upon binding of cognate ligand, Notch protein undergoes a proteolytic cleavage that releases Notch intracellular domain (NICD/Cleaved Notch) that translocates to the nucleus and forms a complex with DNA-binding protein CSL/RBP-Jk and activates specific gene transcription (12). Interestingly, Wnt and Notch signaling pathways are intimately intertwined during self-renewal of stem cells and tumor development. Furthermore, physical binding of Notch to

---

[5] The abbreviations used are: TCF, T cell factor; iNOS, inducible nitric-oxide synthase; NICD, Notch intracellular domain; TBM, tuberculous meningitis; CHAPSO, 3-[(3-cholamidopropyl)dimethylammonio]-2-hydroxy-1-propanesulfonic acid.

β-catenin or their association with common co-factors has been demonstrated in various cellular systems. In addition, accurate coordination of Notch and Wnt signals is critical during normal development (13–15). Intriguingly, many Notch target genes such as cyclooxygenase-2 (*COX-2*), *Jagged1*, and *Hes1* are also targeted by Wnt-β-catenin, suggesting a functional overlap between Notch and Wnt-β-catenin pathways (16–20).

In view of the above observations, we set out to unravel the molecular mechanisms contributing toward pathogen-specific Toll-like receptor responses, principally with respect to the role of Wnt-β-catenin and Notch signaling axis. We demonstrate that "pathogenic" TLR2 stimulation confers differential activation of Wnt-β-catenin signaling in macrophages. Infection with *Mycobacterium bovis* BCG in comparison with *Salmonella typhimurium* and *Staphylococcus aureus* resulted in consistent activation of Wnt-β-catenin signaling at multiple levels, including up-regulation of *Wnt5a* and *FzD4* transcript levels, stabilization of β-catenin, and activation of Wnt-β-catenin transcriptional activity, thus culminating in the expression of a multitude of genetic signatures crucial for mounting appropriate regulatory or tolerogenic responses, including COX-2 and suppressor of cytokine signaling-3 (SOCS-3). Intriguingly, non-pathogenic bacterial strains *Mycobacterium smegmatis* or *Escherichia coli* failed to induce consistent up-regulation of signaling cohorts of the Wnt-β-catenin signaling cascade. *M. bovis* BCG-triggered stabilization of β-catenin led to an increase in its occupancy on genomic targets, including Jagged1 culminating in induced activation of Notch1 signaling. We present the evidence that inducible nitric-oxide synthase (iNOS) activity is a critical factor in TLR2-mediated activation of Wnt-β-catenin signaling as macrophages derived from iNOS knock-out ($iNOS^{-/-}$), but not from wild type (WT) mice, failed to activate Wnt5a/FzD4 expression as well as Notch1 signaling upon *M. bovis* BCG infection. The loss of TLR2-mediated Wnt5a/FzD4 expression or Notch1 activation in $iNOS^{-/-}$ macrophages could be rescued by treatment with the NO donor, 3-morpholinosydnonimine (SIN-1). Correlative evidence infers that this mechanism operates *in vivo* as immunohistochemical expression of β-catenin, Jagged1, activated Notch1, or its target gene products COX-2 and SOCS-3 could be detected in brains derived from wild type (WT) but not $iNOS^{-/-}$ mice that were intracerebrally infected with *M. bovis* BCG. Consistent with these results, activation of Wnt-β-catenin/Notch1 signaling *in vivo* could be demonstrated only in granulomatous lesions in brains derived from human tuberculous meningitis patients as opposed to healthy individuals validating the role of TLR2-dependent activation of the Wnt-Notch signaling axis in mycobacterial pathogenesis. Interestingly, Wnt-β-catenin/Notch signaling dictates T_{Reg} lineage commitment via reprogramming of the gene expression pattern in macrophages, including induced expression of COX-2 and SOCS-3. Thus, these studies establish the Wnt-β-catenin/Notch signaling axis as a determinant of pathogen-specific regulatory TLR2 responses that may play a major role in dictating the functional outcomes of tuberculosis infection.

EXPERIMENTAL PROCEDURES

Cells, Mice, and Bacteria—Peritoneal macrophages were isolated from peritoneal exudates of C57BL/6 or $iNOS^{-/-}$ C57BL/6 or $TLR2^{-/-}$ C57BL/6 mice that were maintained at the central animal facility, Indian Institute of Science. CD4$^+$ T cells were enriched from splenocytes obtained from C57BL/6 mice. The RAW 264.7 mouse macrophage cell line was cultivated in DMEM (Sigma) supplemented with 10% heat-inactivated FBS (Sigma). All studies involving mice were carried out after the approval from the Institutional Ethics Committee for Animal Experimentation and from Institutional Biosafety Committee. *M. bovis* BCG Pasteur 1173P2, *S. typhimurium,* and *S. aureus* were grown to mid-log phase, and batch cultures were aliquoted followed by storage at −70 °C. Representative vials were thawed and enumerated for viable colony-forming units and used at 10 multiplicities of infection for infection in all the experiments.

Reagents and Antibodies—General laboratory chemicals were obtained from Sigma or Merck. Anti-COX-2 and anti-proliferating cell nuclear antigen (PCNA) antibodies were purchased from Calbiochem. Anti-β-actin and anti-PGE$_2$ antibodies were purchased from Sigma. Anti-Ser-338 phospho-Raf1, anti-Raf1, anti-Thr-80/Tyr-182 phospho-p38 MAPK, anti-p38 MAPK, anti-Thr-202/Tyr-204 phospho-ERK1/2, anti-ERK1/2, anti-NF-κB p65, anti-cleaved Notch1 or anti-NICD (Val-1744), anti-Jagged1, anti-α/βII Thr-638/641 phospho-PKC, anti-βII Ser-660 phospho-PKC, anti-δ Thr-505 phospho-PKC, anti-SOCS-3, anti-Wnt5a, anti-Ser-33/37/Thr-41 phospho-β-catenin, anti-β-catenin, anti-Ser-9-phospho-GSK-3β antibodies were purchased from Cell Signaling Technology. Fluorescein isothiocyanate (FITC)-conjugated monoclonal antibodies (mAbs) to CD4 and phycoerythrin-conjugated mAbs to CD25 were from Miltenyi Biotec. Anti-FoxP3 antibodies were purchased from Imgenex. HRP-conjugated anti-rabbit IgG and anti-mouse IgG as well as Cy5-conjugated anti-rabbit IgG antibodies were obtained from Jackson ImmunoResearch.

Treatment with Pharmacological Reagents—All the pharmacological reagents were procured from Calbiochem and were reconstituted in sterile DMSO (Sigma) and used at the following concentrations: β-catenin inhibitor (7.5 or 15 μM), γ-secretase inhibitor-I (GSI-I) (10 μM), chelerythrine (1 μM), RO31-8220 (1 μM), PKCα inhibitor (50 μM), PKCβ inhibitor (20 μM), PKCδ inhibitor (10 μM), PKCε inhibitor (50 μM), PKCζ inhibitor (5 μM), LiCl (10 or 20 mM), IWP-II (5 μM), and SIN-1 (20 μM). DMSO at 0.1% concentration was used as the vehicle control. In all experiments involving pharmacological reagents, a tested concentration was used after careful titration experiments assessing the viability of the macrophages using 3-(4,5-dimethylthiazol-2-yl)-2,5 diphenyltetrazolium bromide assay. In experiments with inhibitors, the cells were treated with a given inhibitor for 60 min before experimental treatment.

RNA Isolation and Quantitative Real Time PCR—Macrophages were infected with individual bacterial strain as indicated, and total RNA from infected macrophages was isolated utilizing TRI Reagent® (Sigma), as per the manufacturer's protocol, and treated with RNase-free DNase (Promega). The

cDNA synthesis kit (Fermentas) was used for reverse transcription according to the manufacturer's protocol. A real time PCR amplification (Applied Biosystems) using SYBR Green PCR mix (Finnzymes, Finland) was performed for quantification of target gene expression. All the experiments involving real time PCR amplification were repeated at least three times independently to ensure the reproducibility of the results. Amplification of housekeeping gene *GAPDH* was used as internal control. Primer sequences used in the current study are as follows: *GAPDH* forward 5′-gagccaaacgggtcatcatct-3′, *GAPDH* reverse 5′-gaggggccatccacagtctt-3′; *COX-2* forward 5′-gtatcagaaccgcattgcctc-3′, *COX-2* reverse 5′-cggcttccagtattgaggagaacagat-3′; *SOCS-3* forward 5′-gcgagaagattccgctggta-3′, *SOCS-3* reverse 5′-ccgttgacagtcttccgacaa-3′; *Wnt1* forward 5′-ggtttctactacgttgctactgg-3′, *Wnt1* reverse 5′-ggaatccgtcaacaggttcgt-3′; *Wnt2a* forward 5′-ctcggtggaatctggctctg-3′, *Wnt2a* reverse 5′-cacattgtcacacatcaccct-3′; *Wnt2b* forward 5′-tgtgtcaacgctaccagac-3′, *Wnt2b* reverse 5′-gtccagtgtggtgcaattcca-3′; *Wnt3a* forward 5′-tggctgagggtgtcaaagc-3′, *Wnt3a* reverse 5′-cgtgtcactgcgaaagctact-3′; *Wnt4* forward 5′-agacgtgcgagaaactcaaag-3′, *Wnt4* reverse 5′-ggaactggtattggcactcct-3′; *Wnt5a* forward 5′-tgcggagacaacatcgactat-3′, *Wnt5a* reverse 5′-tccatgacacttacaggctaca-3′; *Wnt5b* forward 5′-ctgctgactgacgccaact-3′, *Wnt5b* reverse 5′-cctgatacaactgacacagcttt-3′; *Wnt6* forward 5′-atgtggacttcggggatgaga-3′, *Wnt6* reverse 5′-gcctcgttgttgtgcagttg-3′; *Wnt7a* forward 5′-cctggacgagtgtcagtttca-3′, *Wnt7a* reverse 5′-cccgactcccacttttgag-3′; *Wnt7b* forward 5′-atcgactttctcgtcgcttt-3′, *Wnt7b* reverse 5′-cgtgacacttacattccagctc-3′; *Wnt8a* forward 5′-ctccagactcttcgtggacag-3′, *Wnt8a* reverse 5′-acacttgcaggtcctttcgt-3′; *Wnt8b* forward 5′-aaggcttacctggtctactcc-3′, *Wnt8b* reverse 5′-ctctctcggggcaattccaa-3′; *Wnt9a* forward 5′ acacctggacgactctccc-3′, *Wnt9a* reverse 5′-cttgtcaccacacgactctgt-3′; *Wnt9b* forward 5′-agaggctttaaggagacggc-3′, *Wnt9b* reverse 5′-ggggagtcgtcacaagtacag-3′; *Wnt10b* forward 5′-gagggtagtggtgagcaaga-3′, *Wnt10b* reverse 5′-ggttacagccaccccattcc-3′; *Wnt11* forward 5′-tcatgggggccaagttttcc-3′, *Wnt11* reverse 5′-ttccagggaggcagtagag-3′; *FzD4* forward 5′-tcctgagagaatttgggtttgc-3′, *FzD4* reverse 5′-ggctggatgggagtcttgtg-3′; *LRP5* forward 5′-ctatccgcagggcgtaccta-3′, *LRP5* reverse 5′-cgagtcacctcaattctgtcag-3′; *Notch1* forward 5′-agaatggcatggtgcccag-3′, *Notch1* reverse 5′-tggtggagaggctgctgtgtag-3′; and *Jagged1* forward 5′-agaagtcagagttcagaggcgtcc-3′, *Jagged1* reverse 5′-agtagaaggctgtcaccaagcaac-3′.

Immunoblotting—Macrophages were washed twice with PBS, scraped off the culture dish, and collected by centrifugation. Cell lysates were prepared in RIPA buffer consisting of 50 mM Tris-HCl (pH 7.4), 1% Nonidet P-40, 0.25% sodium deoxycholate, 150 mM NaCl, 1 mM EDTA, 1 mM PMSF, 1 μg/ml each of aprotinin, leupeptin, pepstatin, 1 mM Na_3VO_4, 1 mM NaF and incubated on ice for 30 min. Whole cell lysate was collected by centrifuging lysed cells at 13,000 × *g* for 10 min at 4 °C. An equal amount of protein from each cell lysate was subjected to SDS-PAGE and transferred onto PVDF membranes (Millipore) by semidry Western blotting (Bio-Rad) method. Nonspecific binding was blocked with 5% nonfat dry milk powder in TBST (20 mM Tris-HCl (pH 7.4), 137 mM NaCl, and 0.1% Tween 20) for 60 min. The blots were incubated overnight at 4 °C with primary antibodies diluted in TBST with 5% BSA. After washing with TBST, blots were incubated with anti-rabbit or anti-mouse IgG secondary antibodies conjugated to HRP for 2 h. After further washing in TBST, the immunoblots were developed with enhanced chemiluminescence detection system (PerkinElmer Life Sciences) as per manufacturer's instructions.

Nuclear and Cytosolic Subcellular Fractionation—Macrophages were treated as indicated, harvested by centrifugation, and gently resuspended in ice-cold Buffer A (10 mM HEPES (pH 7.9), 10 mM KCl, 0.1 mM EDTA, 0.1 mM EGTA, 1 mM DTT, and 0.5 mM PMSF). After incubation on ice for 15 min, cell membranes were disrupted with 10% Nonidet P-40, and the nuclear pellets were recovered by centrifugation 13,000 × *g* for 15 min at 4 °C. The supernatants from this step were used as cytosolic extracts. Nuclear pellets were lysed with ice-cold Buffer C (20 mM HEPES (pH 7.9), 0.4 M NaCl, 1 mM EDTA, 1 mM EGTA, 1 mM DTT, and 1 mM PMSF), and nuclear extracts were collected after centrifugation at 13,000 × *g* for 20 min at 4 °C.

Enzyme Immunoassay for PGE2—Enzyme immunoassays for quantification of PGE_2 in culture supernatant of treated samples were carried out in 96-well microtiter plates using PGE_2 Express EIA kit (Cayman Chemical). Assay plates were incubated with culture supernatants and processed according to the manufacturer's instructions. The absorbance was measured at 420 nm using enzyme-linked immunosorbent assay (ELISA) reader (Molecular Devices).

Measurement of Nitric Oxide—To measure the amount of NO produced by macrophages, macrophages were treated as indicated. At the end of experiment, culture supernatants were harvested by centrifugation and subjected to assay for NO production using Griess reagent according to the manufacturer's instructions (Promega).

γ-Secretase Activity Assay—To measure γ-secretase activity, solubilized cell membranes were incubated in 150 μl of assay buffer containing 50 mM Tris-HCl (pH 6.8), 2 mM EDTA, 0.25% CHAPSO (w/v), and 8 μM fluorogenic γ-secretase peptide substrate (Calbiochem) at 37 °C for 12 h. After incubation, samples were centrifuged at 13,000 × *g* for 15 min followed by measurement of fluorescence using a fluorometer with excitation wavelength at 355 nm and emission wavelength at 440 nm.

Transfection Studies—RAW 264.7 macrophage cells were transfected with 100 nM siRNA using Oligofectamine (Invitrogen) according to the manufacturer's instructions. Transfection efficiency has been more than 50% through all the experiments as determined by counting the number of siGLO Lamin A/C-positive cells in a microscopic field using a fluorescent microscope. 72 h post-transfection, the cells were treated as indicated and processed for expression analysis. Wnt5a, β-catenin, Notch1, MyD88, and control siRNAs were obtained from Dharmacon as siGENOME™ SMARTpool reagents, which contains a pool of four different double-stranded RNA oligonucleotides (siRNA). RAW 264.7 macrophages were transiently transfected with PKCα, PKCβ, and PKCδ dominant negative cDNA constructs using low molecular weight polyethyleneimine (Sigma).

Chromatin Immunoprecipitation Assay—Chromatin immunoprecipitation (ChIP) assays were carried out using protocol

provided by Upstate Biotechnology, Inc., with certain modifications. Briefly, mouse macrophages were infected with *M. bovis* BCG for 6 h. The cells were fixed with 1.42% formaldehyde for 15 min at room temperature followed by inactivation of formaldehyde with addition of 125 mM glycine. Chromatin extracts containing DNA fragments with an average size of 500 bp were immunoprecipitated using anti-β-catenin antibodies. Purified DNA was analyzed by quantitative PCR using the SYBR Green method (Finnzymes, Finland). Regions with β-catenin/TCF-binding site in mouse *Jagged1* promoter were amplified using primer pairs, β-catenin/TCF forward, 5′-cctccccgcgtttcatg-3′, β-catenin/TCF reverse, 5′-gcaaagagcccggcctc-3′; 28 S rRNA was used as control in the PCR and the primers were forward 5′-ctgggtataggggcgaaagac-3′ and reverse 5′-ggccccaagacctctaatcat-3′. All results were normalized either by respective input values or by amplification of 28 S rRNA. All ChIP experiments were repeated at least three times.

Tuberculosis Patients and Healthy Subjects—The study population was comprised of tuberculous meningitis patients (TBM, $n = 24$), pulmonary tuberculosis patients ($n = 11$), and healthy controls ($n = 4$) reporting to the National Institute of Mental Health and Neurosciences, Bangalore, India. TBM patients were described as having clinical meningitis along with culture positivity for acid-fast bacilli and/or *M. tuberculosis* cultured from the cerebrospinal fluid. Active pulmonary tuberculosis disease in patients was established by detection of acid-fast bacilli in sputum smear examinations or growth of bacilli in BACTEC cultures. Patients with active pulmonary tuberculosis infection were also examined for radiological abnormalities by chest x-ray. The healthy subjects included in the study were recruited after radiological and clinical examination to exclude individuals with active tuberculosis disease. The study subjects had given written consent, and the study was approved by the Institutional Bioethics Committee.

In Vivo Challenge of Mice with M. bovis BCG or SIN-1—C57BL/6 and *iNOS$^{-/-}$* C57BL/6 mice used in the current investigation were 5–6 weeks old, and each *in vivo* experiment involved three animals per group. For intracerebral infection, 1×10^6 *M. bovis* BCG Pasteur 1173P2 bacteria were washed in PBS, resuspended in 50 μl of sterile PBS, followed by intracranial inoculation using 1-ml syringes and a 26-gauge needle. Control mice received 50 μl of sterile PBS using the same protocol. One set of *iNOS$^{-/-}$* mice were inoculated with 20 μg of SIN-1. Before intracranial inoculation, mice were anesthetized with intraperitoneal injection of ketamine (6 mg). In experiments involving TLR2 antibody, WT mice received anti-TLR2 or control IgG antibody (200 μg/kg) 24 h prior to infection with *M. bovis* BCG (18, 21). For *in vivo* knockdown of MyD88, WT mice were injected with 0.6 nmol of MyD88 or control siRNA complexed with low molecular weight polyethyleneimine 24 h before intracranial inoculation with *M. bovis* BCG (18, 22–24). After 5 days of inoculation, brains were harvested from experimental mice and processed for either tissue sectioning or RNA isolation.

Immunohistochemistry—Microtome sections (4μm) were sliced from formalin-fixed, decalcified, and paraffin-embedded tissue samples. These paraffin-embedded sections were first

deparaffinized, followed by antigen retrieval with boiling 10 mM citrate buffer (pH 6.0) in a boiling water bath for 10 min, treated with 1% H_2O_2 for 10 min, and blocked with 5% BSA for 1 h at room temperature. The tissue sections were incubated with primary antibodies for 12 h and HRP-conjugated secondary antibodies for 90 min. The horseradish peroxidase reaction was detected with 0.05% diaminobenzidine and 0.03% H_2O_2. Sections were counterstained with hematoxylin, dehydrated, and mounted. Stained tissue sections were analyzed with a Leica DMLB microscope (Leica Microsystems, Wetzlar, Germany). All experiments were performed with appropriate isotype-matched control Abs.

Detection of CD4$^+$CD25$^+$FoxP3$^+$ T$_{Reg}$ Cells by Flow Cytometry—Macrophages were treated as indicated for 24 h followed by co-culture with enriched CD4$^+$ T cells for 5 days at 37 °C in a humidified 5% CO_2 atmosphere. Surface and intracellular staining to detect CD4$^+$CD25$^+$Foxp3$^+$ T$_{Reg}$ cells was performed with specifically labeled mAbs, and samples were proceeded for flow cytometry (LSR II, BD Biosciences). Cells were gated for CD4$^+$ lymphocytes followed by determination of the percentages of CD25$^+$Foxp3$^+$ cells. For each sample, five thousand events were recorded. Data were analyzed using BD FACS DIVA software (BD Biosciences).

Statistical Analysis—Levels of significance for comparison between samples were determined by the Student's *t* test distribution. The data in the graphs are expressed as the mean ± S.E. *p* values < 0.05 were defined as significant. Graphpad Prism 3.0 software (Graphpad Software) was used for all the statistical analysis.

RESULTS

Pathogen-specific TLR2 Signaling Controls Activation of Wnt-β-Catenin and Notch1 Signaling—Wnt5a, a prototypical member of Wnt family, is induced by LPS/IFN-γ in human macrophages and has been critically implicated in inflammatory macrophage signaling in sepsis and various other pathophysiological diseases, including tuberculosis (25, 26). Interestingly, Wnt5a has long been considered to be a representative noncanonical Wnt in several cell types. However, recent reports have indicated that Wnt5a can activate discrete β-catenin signaling in the presence of FzD4 and LRP5 (27, 28). Furthermore, during the initial stages of this study, we had performed extensive screening in regard to expression levels of various members of Wnt family upon infection of macrophages with *M. bovis* BCG in comparison with nonpathogenic bacterial strains *M. smegmatis* or *E. coli*. As demonstrated in supplemental Fig. S1A, infection with *M. bovis* BCG led to robust up-regulation of *Wnt5a* in comparison with other prototypical members of Wnt family, including *Wnt3a*. Interestingly, nonpathogenic microbial species, *M. smegmatis* and *E. coli*, failed to trigger consistent up-regulation of Wnt5a or other members of Wnt family suggesting a close nexus between Wnt5a and pathogenic *versus* nonpathogenic immune responses.

Interestingly, activation of pathogenic TLR2 signaling upon infection with *M. bovis* BCG, in comparison with other pathogenic microbes, including *S. typhimurium* and *S. aureus*, resulted in robust expression of FzD4 and LRP5 in
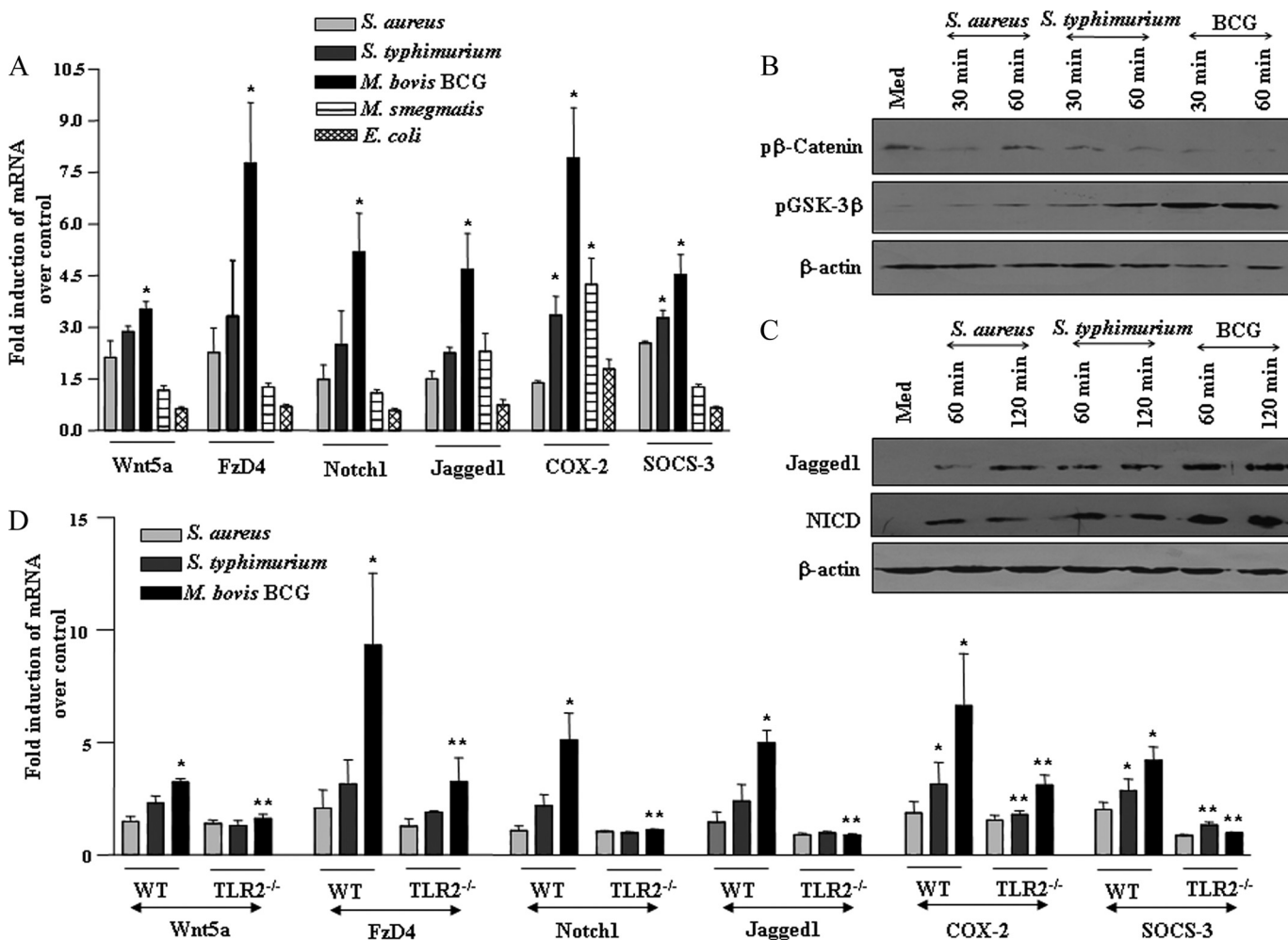
FIGURE 1. **Pathogen-specific TLR2 signaling shapes the activation of Wnt-β-catenin and Notch1 pathway.** *A,* mouse macrophages were infected with 1:10 multiplicity of infection of *S. aureus, S. typhimurium, M. bovis* BCG, *M. smegmatis,* or *E. coli* and transcript levels of *Wnt5a, FzD4, Notch1, Jagged1, COX-2,* and *SOCS-3* were analyzed by quantitative real time PCR (mean ± S.E., n = 3). *B* and *C,* pathogen-specific increase in phosphorylation of GSK-3β and concomitant decrease in phosphorylation of β-catenin (*B*) as well as augmentation in expression of Jagged1 and NICD upon infection with *S. aureus, S. typhimurium,* or *M. bovis* BCG (*C*). *D,* macrophages derived from TLR2$^{-/-}$ mice exhibit the impaired ability to trigger expression of *Wnt5a, FzD4, Notch1, Jagged1, COX-2,* and *SOCS-3* upon infection with *S. aureus, S. typhimurium,* or *M. bovis* BCG (mean ± S.E., n = 3). The data are representative of three independent experiments. *Med,* medium; *WT,* wild type. *, $p < 0.05$ *versus* control; **, $p < 0.05$ *versus* WT.

addition to Wnt5a in macrophages (Fig. 1*A* and supplemental Fig. S1, *B–D*). Activation of canonical Wnt signaling is characterized by increased levels of phosphorylated GSK-3β with a concomitant decrease in phosphorylated β-catenin (8). Accordingly, infection of macrophages with *M. bovis* BCG triggered significant increase and concomitant decrease in phosphorylation of GSK-3β and β-catenin, respectively, compared with *S. typhimurium* or *S. aureus* challenge (Fig. 1*B*).

As described previously, Wnt signaling-regulated cell fate decisions often involve the activation of Notch1 signaling, and we have previously demonstrated that *M. bovis* BCG challenge provokes spectrum of cellular signaling, including Notch signaling activation (16, 18, 19). Evidently, Notch target genes are often regulated by Wnt-β-catenin, thus suggesting a role for integrated signaling circuits in modulation of immune responses (17, 20). Consistent with these observations, *M. bovis* BCG infection compared with *S. typhimurium* or *S. aureus* triggered robust activation of Notch1 signaling as evidenced by induced expression of Notch1, its cognate receptor Jagged1,

generation of NICD, and enhanced expression of Notch1 target gene products, COX-2 and SOCS-3 (Fig. 1, *A* and *C*, and supplemental Fig. S1*E*).

Furthermore, the ability of *M. bovis* BCG to trigger activation of Wnt-β-catenin and Notch1 signaling required participation of TLR2 as macrophages derived from TLR2$^{-/-}$ mice exhibited impaired ability to trigger expression of Wnt5a, FzD4, Notch1, Jagged1, COX-2, and SOCS-3 (Fig. 1*D*). Interestingly, non-pathogenic microbial species, *M. smegmatis* and *E. coli,* failed to trigger consistent up-regulation of signaling mediators of Wnt-β-catenin and Notch1 signaling (Fig. 1*A* and supplemental Fig. 1*F*).

Activation of Wnt-β-Catenin and Notch1 Signaling during Human Tuberculosis Infection—To bring relevance to the biology of *Mycobacterium* infection *in vivo,* we investigated the expression of various cohorts of Wnt-β-catenin and Notch1 signaling in peripheral blood mononuclear cells derived from tuberculosis patients. Transcript level analysis demonstrated higher levels of *Wnt5a, FzD4, Notch1,* and *Jagged1* as well as its target genes *COX-2* and *SOCS-3* in *M.*
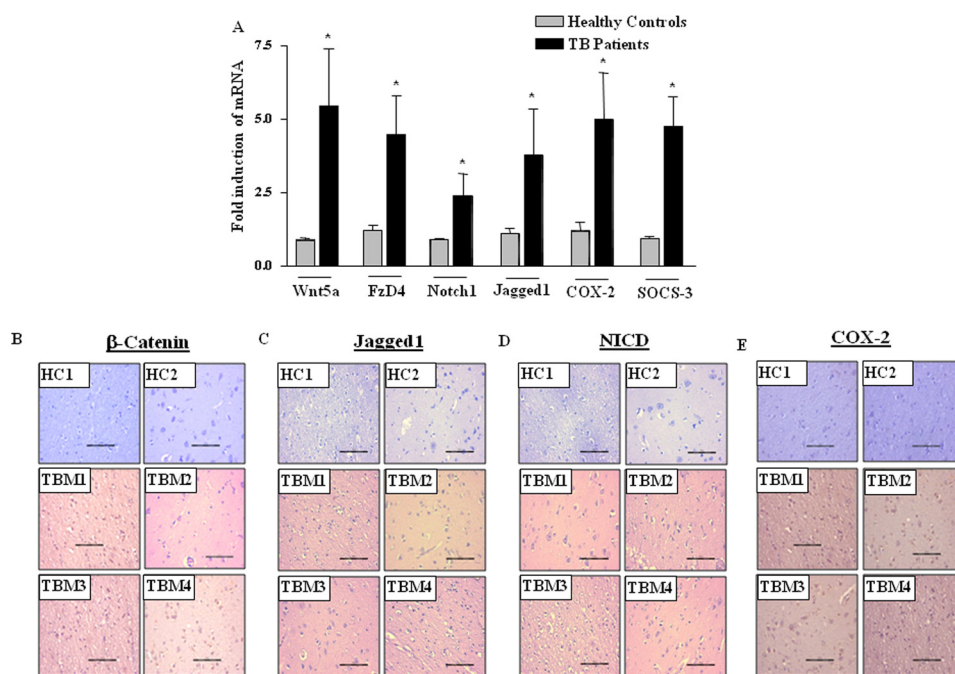
FIGURE 2. **Activation of Wnt-β-catenin and Notch1 pathway in human tuberculosis patients.** *A*, induced expression of *Wnt5a, FzD4, Notch1, Jagged1, COX-2,* and *SOCS-3* in peripheral blood mononuclear cells from pulmonary tuberculosis patients in comparison with healthy subjects (mean ± S.E., $n = 4$ (*healthy controls*), $n = 11$ (*TB patients*)). *B–E*, serial sections of human brain tissue samples of TBM patients or healthy subjects were stained for expression levels of β-catenin (*B*), Jagged1 (*C*), activated Notch1/NICD (*D*), and COX-2 (*E*). Hematoxylin (*blue*) was used for nuclear staining. *Scale bar,* 100 μm. *HC,* healthy control; *TBM,* tuberculous meningitis; *TB*, tuberculosis. *, $p < 0.05$ *versus* healthy controls.
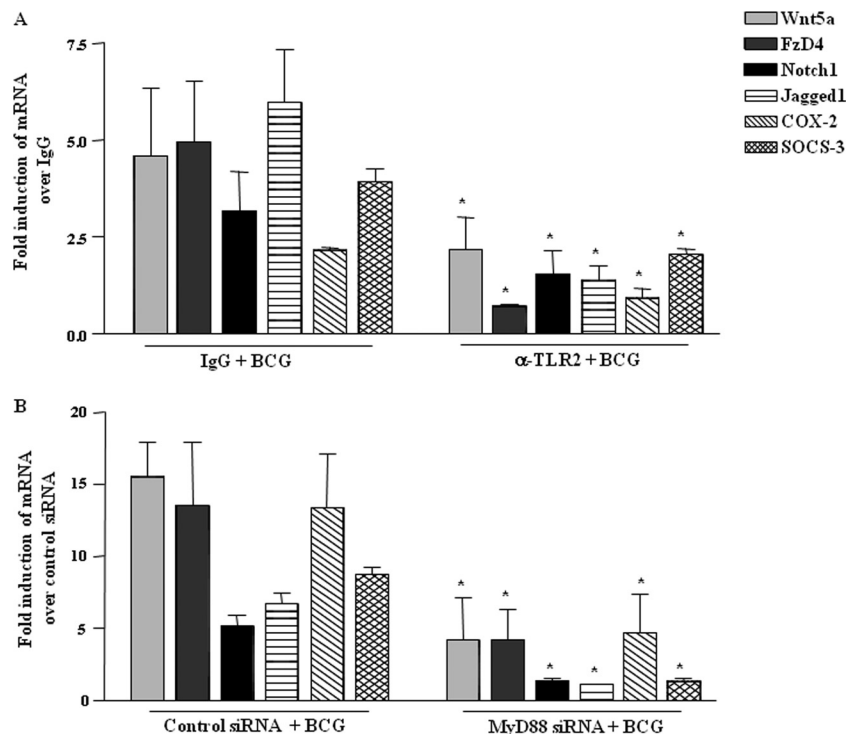

FIGURE 3. **Mycobacteria activate Wnt-β-catenin and Notch1 pathway in TLR2-dependent manner *in vivo*.** *A*, WT mice were injected with anti-TLR2 or control IgG antibody 24 h before intracranial inoculation with *M. bovis* BCG and expression of *Wnt5a, FzD4, Notch1, Jagged1, COX-2,* and *SOCS-3* was analyzed by quantitative real time PCR (mean ± S.E., $n = 3$ mice from three independent experiments). *B*, expression analysis of *Wnt5a, FzD4, Notch1, Jagged1, COX-2,* and *SOCS-3* in brain tissue of WT mice injected with *MyD88* or control siRNA complexed with polyethyleneimine 24 h prior to intracranial inoculation with *M. bovis* BCG (mean ± S.E., $n = 3$ mice from two to three independent experiments). Each experimental group involved three mice per experiment. *WT,* wild type. *, $p < 0.05$ *versus* IgG + BCG or control siRNA + BCG.

tuberculosis-infected individuals in comparison with healthy subjects (Fig. 2*A*). In addition, immunohistochemical expression analysis of brain tissue samples from TBM patients exhibited significantly increased expression levels of β-catenin, Jagged1, or NICD compared with healthy subjects (Fig. 2, *B–D*). Similarly, COX-2 expression levels were
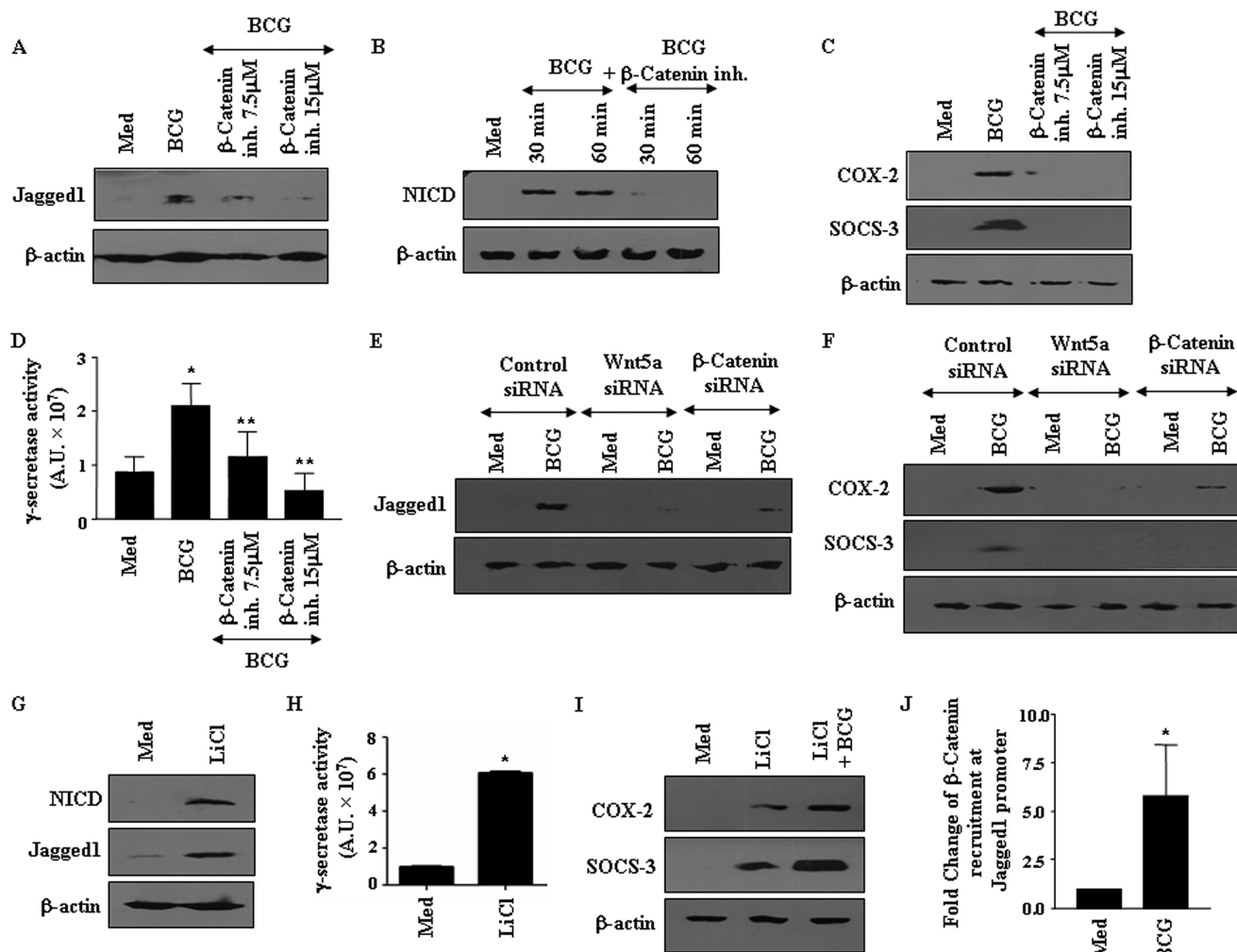
FIGURE 4. **Wnt-β-catenin signaling is essential for activation of Notch1 cascade.** *A–C*, inhibition (*inh*) of β-catenin activity abolished *M. bovis* BCG-induced expression of Jagged1 (*A*), NICD (*B*), and COX-2 and SOCS-3 (*C*). *D*, pretreatment of macrophages with β-catenin inhibitor abrogated *M. bovis* BCG-triggered activity of γ-secretase complex. *E* and *F*, siRNA-mediated knockdown of *Wnt5a* and β-catenin blocked *M. bovis* BCG-triggered expression of Jagged1 (*E*) and COX-2 and SOCS-3 (*F*). *G* and *H*, treatment of macrophages with 10 mM LiCl augmented expression of NICD and Jagged1 (*G*) and activity of γ-secretase complex (*H*). *I*, infection with *M. bovis* BCG augments LiCl-triggered expression of COX-2 and SOCS-3. *J*, recruitment of β-catenin/TCF at mouse Jagged1 promoter upon infection with *M. bovis* BCG was assessed by chromatin immunoprecipitation assay. *Error bars* represent mean ± S.E. (*n* = 3). Data are representative of three independent experiments. *Med*, medium. *, *p* < 0.05 *versus* medium; **, *p* < 0.05 *versus* BCG.

significantly enhanced in brain samples of TBM patients compared with healthy subjects (Fig. 2*E*).

Pathogenic TLR2-MyD88 Axis Is an Essential Link in M. bovis BCG-triggered Activation of Wnt-β-Catenin and Notch1 Signaling in Vivo in Mice—To establish contribution of pathogenic TLR2-MyD88 axis in activation of Wnt-β-catenin and Notch1 signaling *in vivo*, a suggested murine model for the study of CNS tuberculosis or tuberculous meningitis involving intracranial inoculation of *M. bovis* BCG was utilized (29). Selective interference with TLR2 signaling *in vivo* by neutralizing antibodies against TLR2 clearly abrogated *M. bovis* BCG-triggered Wnt5a, FzD4, Notch1, and Jagged1 expression as well as expression of Notch1 signaling target genes COX-2 and SOCS-3 (Fig. 3*A*). Accordingly, siRNA-mediated knockdown of MyD88 *in vivo* abolished *M. bovis* BCG-induced expression of signaling intermediates of Wnt-β-catenin and Notch1 signaling, including Wnt5a, FzD4, Jagged1, and Notch1 or its target genes COX-2 and SOCS-3 (Fig. 3*B*). These results strongly advocate a critical role for

TLR2-MyD88 axis in activation of Wnt-β-catenin and Notch1 signaling *in vivo*.

Jagged1 Is Pathogenic Link between M. bovis BCG-triggered Wnt-β-Catenin and Notch1 Pathways—Wnt-β-catenin pathway can directly influence diverse signaling cascades through activation of specific genetic signatures, including Jagged1-driven activation of Notch1 (20). In view of robust activation of Wnt-β-catenin and Notch1 pathways during pathogen-specific activation of TLR2 signaling by mycobacteria, identification of possible cross-talk between these signaling pathways assumes novel significance. In this perspective, pharmacological inhibition of β-catenin activity significantly abolished *M. bovis* BCG-triggered Jagged1 expression as well as activation of Notch1 (Fig. 4, *A* and *B*). Accordingly, expression of Notch1 target genes, COX-2, SOCS-3, as well as PGE$_2$, an immunosuppressive product of COX-2 activity, was inhibited by β-catenin inhibitor (Fig. 4*C* and supplemental Fig. S2*A*). Furthermore, activation of Notch1 signaling is tightly regulated by protease activity executed by γ-secretase complex that releases the
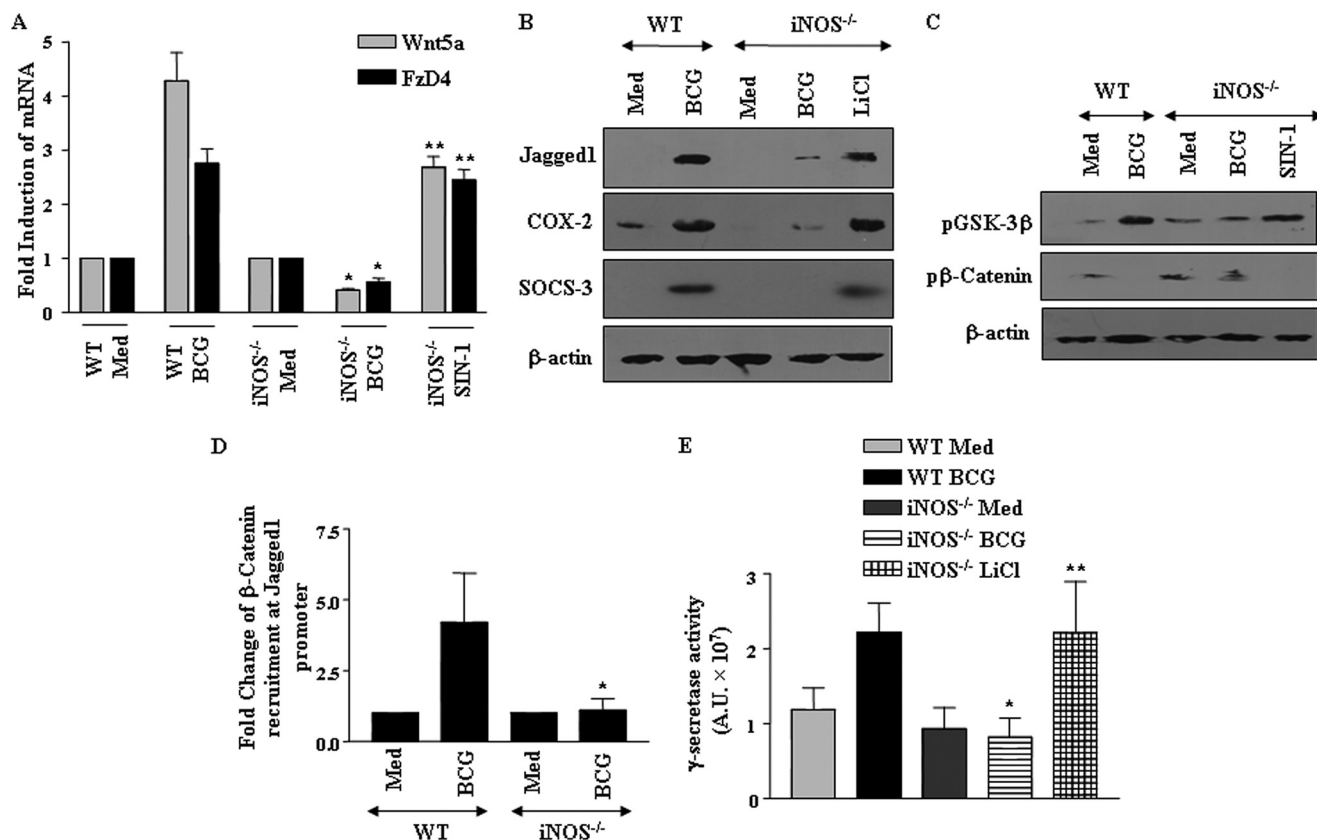
FIGURE 5. **Requirement of iNOS/NO in *M. bovis* BCG-dependent signaling integration of Wnt-β-catenin and Notch1 cascade.** *A*, macrophages derived from WT mice were infected with *M. bovis* BCG, and *iNOS*^−/− macrophages were either infected with *M. bovis* BCG or treated with SIN-1 and analyzed for expression of Wnt5a and FzD4 by quantitative real time PCR. *B*, expression levels of Jagged1, COX-2, and SOCS-3 in WT and *iNOS*^−/− macrophages infected with *M. bovis* BCG and *iNOS*^−/− macrophages treated with LiCl. *C*, *iNOS*^−/− macrophages failed to induce activation of β-catenin and concomitant inhibition of GSK-3β. SIN-1 treatment of *iNOS*^−/− macrophages rescued its impaired ability to activate β-catenin and inhibit GSK-3β. *D*, recruitment of β-catenin/TCF at mouse Jagged1 promoter was analyzed by chromatin immunoprecipitation assay with antibodies to β-catenin in *M. bovis* BCG-infected WT or *iNOS*^−/− macrophages. *E*, analysis of γ-secretase activity in WT macrophages infected with *M. bovis* BCG or *iNOS*^−/− macrophages challenged with either *M. bovis* BCG or LiCl. The results in *bar graphs* are expressed as mean ± S.E. of three independent experiments, and the blots are representative of three independent experiments. *Med*, medium; *WT*, wild type. *, $p < 0.05$ *versus* WT BCG; **, $p < 0.05$ *versus* *iNOS*^−/− BCG.

active NICD (12). Significantly, pharmacological inhibition of β-catenin strongly repressed *M. bovis* BCG-triggered γ-secretase activity (Fig. 4*D*). Furthermore, siRNA-mediated knockdown of Wnt5a and β-catenin severely compromised *M. bovis* BCG-elicited expression of Jagged1, NICD, as well as COX-2 and SOCS-3 (Fig. 4, *E* and *F*, and supplemental Fig. S2*B* and data not shown). Moreover, stabilization of β-catenin in macrophages by treatment with the GSK-3β inhibitor LiCl was sufficient to induce Jagged1 expression and enhance γ-secretase complex activity as well as NICD generation (Fig. 4, *G* and *H*). Similarly, LiCl treatment augmented COX-2, SOCS-3, and PGE₂ expression, and infection with *M. bovis* BCG further potentiated LiCl-induced expression of COX-2 and SOCS-3 (Fig. 4*I* and supplemental Fig. S2*C*).

To further validate this, we identified eight sites for β-catenin/TCF binding consensus in mouse *Jagged1* promoter, and chromatin immunoprecipitation analysis revealed that *M. bovis* BCG infection results in enhanced recruitment of β-catenin at the *Jagged1* promoter *in vivo* (Fig. 4*J*). Furthermore, gel shift experiments showed an increased binding of nuclear proteins to β-catenin/TCF consensus in Jagged promoter upon infection with *M. bovis* BCG, which was compromised upon pretreatment of macrophages with β-catenin

inhibitor (supplemental Fig. S2*D*). Concomitantly, LiCl treatment also induced enhanced binding of β-catenin/TCF to its consensus (supplemental Fig. 2*D*). These findings noticeably support the critical participation of the Wnt-β-catenin pathway in *M. bovis* BCG-induced Jagged1 expression and activation of Notch1 signaling in macrophages.

Requirement of iNOS/NO in M. bovis BCG-driven Activation of Wnt-Notch1 Signaling Axis—Nitric oxide (NO), a catalytic product of iNOS, frequently executes critical cell fate decisions by functioning as an important molecular signal in regulation of specific proinflammatory responses in macrophages (30, 31). In this regard, we had earlier reported that iNOS/NO could trigger the activation of Notch1 signaling as well as expression of its target genes, including COX-2 and MMP-9, during *M. bovis* BCG infection (16, 18). Interestingly, iNOS/NO was reported to act as a critical regulator of Wnt signaling responses in a murine model of colitis (32). In this perspective, we addressed whether *M. bovis* BCG-specific activation of TLR2/iNOS/NO axis participates in activation of Wnt-Notch1 signaling. When analyzed, infection with *M. bovis* BCG triggered robust increase in NO levels in comparison with *M. smegmatis*- and *E. coli*-infected macrophages (supplemental Fig. S3*A*). Furthermore, as shown in Fig. 5, *A* and *B*, and supplemental Fig. S3, *B* and *C*,
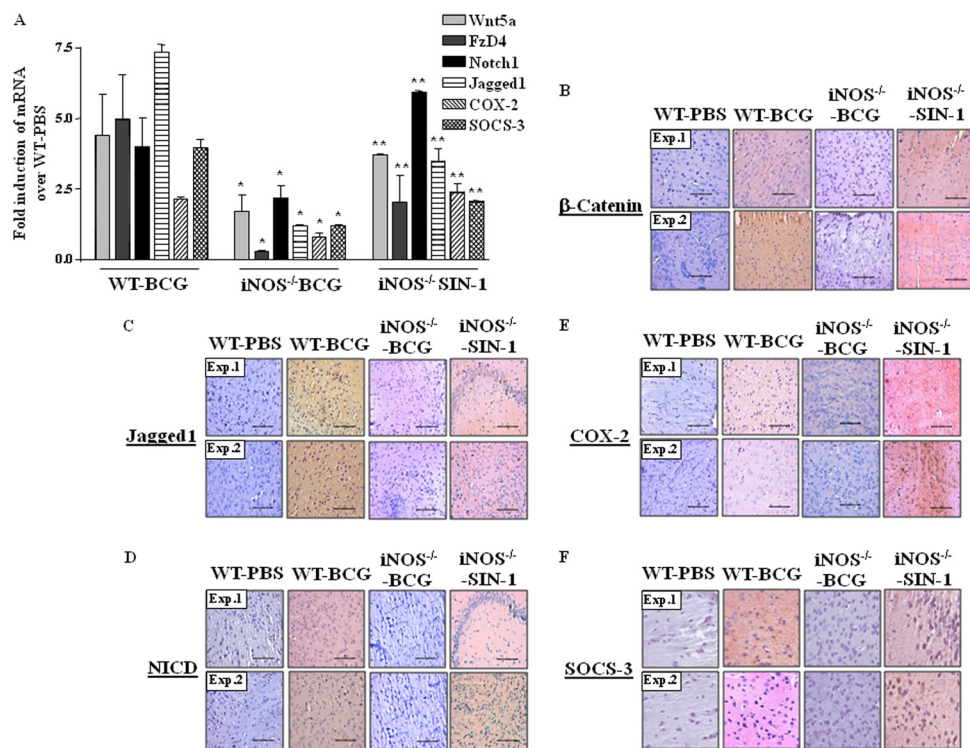
FIGURE 6. **NO acts as mobile signal critical for activation of Wnt-β-catenin and Notch1 signaling *in vivo*.** *A*, brain tissue from WT mice infected with *M. bovis* BCG or *iNOS*$^{-/-}$ mice inoculated with SIN1 in addition to infection with *M. bovis* BCG intracranially were assessed for expression of Wnt5a, FzD4, Notch1, Jagged1, COX-2, and SOCS-3 by quantitative real time PCR (mean ± S.E., *n* = 3 mice from three independent experiments). *B–F*, brain tissue sections from WT or *iNOS*$^{-/-}$ treated experimentally as in *A*, were analyzed for expression levels of β-catenin (*B*), Jagged1 (*C*), NICD (*D*), COX-2 (*E*), and SOCS-3 by immunohistochemistry (*F*). Hematoxylin (*blue*) was used for nuclear staining. The *scale bar* represents 100 μm. Each experimental group involved three mice per experiment. *WT*, wild type. *, *p* < 0.05 *versus* WT BCG; **, *p* < 0.05 *versus iNOS*$^{-/-}$ BCG.

macrophages from iNOS null mice exhibited marked deficiency in *M. bovis* BCG-triggered expression of Wnt5a, FzD4, LRP5, and Jagged1 as well as Notch1 target genes SOCS-3, COX-2, and its bioactive product PGE$_2$, when compared with WT macrophages. Accordingly, deficiency in iNOS expression resulted in marked inhibition in phosphorylation of GSK-3β, concomitant decrease in phosphorylation of β-catenin, and recruitment of β-catenin at Jagged1 promoter (Fig. 5, *C* and *D*). These results are consistent with decreased activity of γ-secretase complex in *iNOS*$^{-/-}$ macrophages (Fig. 5*E* and supplemental Fig. S3*D*). Importantly, deficiency in activation of Wnt-Notch1 signaling was not due to global impairment in diverse cellular functions in iNOS null macrophages as analogues of the iNOS downstream mediator, SIN-1 (NO donor), could restore the activation of various signaling cohorts of Wnt-Notch1 signaling as well as γ-secretase complex in *iNOS*$^{-/-}$ macrophages (Fig. 5, *A* and *C*, and supplemental Fig. S3, *B, D, and E*). Moreover, inhibition of GSK-3β by LiCl in iNOS null macrophages not only activated canonical Wnt-β-catenin signaling as evidenced by stabilized β-catenin levels (supplemental Fig. S3*F*), but it also enhanced expression of Notch1 ligand, Jagged1, and Notch1 target genes COX-2 and SOCS-3 (Fig. 5*B*). Similarly, we observed augmented activation of γ-secretase complex in *iNOS*$^{-/-}$ macrophages upon inhibition of GSK-3β by LiCl (Fig. 5*E*). These results indicate the decisive role of iNOS/NO axis during mycobacterium-specific integration of Wnt-β-catenin and Notch1 signaling.

iNOS/NO Is a Critical Link in Mycobacterium-specific Activation of Wnt-Notch1 Signaling in Vivo—To ascertain the critical role of iNOS/NO axis in TLR2-driven activation of Wnt-Notch1 signaling *in vivo*, WT and *iNOS*$^{-/-}$ mice were challenged intracranially with *M. bovis* BCG, and the activation status of Wnt-β-catenin and Notch1 signaling was analyzed. In accordance with results obtained with macrophages, iNOS deficiency in *iNOS*$^{-/-}$ mice severely compromised the *M. bovis* BCG potential to trigger augmented expression of Wnt5a, FzD4, β-catenin, Jagged1, and Notch1/NICD as evaluated by quantitative real time PCR or immunohistochemistry-based quantifications in the brain sections (Fig. 6, *A–D*). Similarly, expression levels of Notch1 target genes COX-2 or SOCS-3 were markedly reduced in brain sections derived from infected *iNOS*$^{-/-}$ mice compared with WT mice (Fig. 6, *A, E, and F*). Importantly, NO donor (SIN-1) treatment of *iNOS*$^{-/-}$ mice *in vivo* restored expression of Wnt5a, FzD4, β-catenin, Jagged1, and Notch1 as well as Notch1 target genes COX-2 and SOCS-3 (Fig. 6, *A–F*). These results serve as correlative evidence for the role of iNOS/NO in regulation of TLR2-mediated cellular responses, including activation of Wnt-β-catenin and Notch1 signaling.

PKC-MAPK-NF-κB Axis Orchestrates Mycobacterium-specific TLR2 Responses in a Wnt-Notch1-dependent Manner—Protein kinase C (PKC) is suggested to act as a critical regulatory kinase and to effect profound changes in cell physiology by eliciting a transcriptional response and altering the mRNA pro-
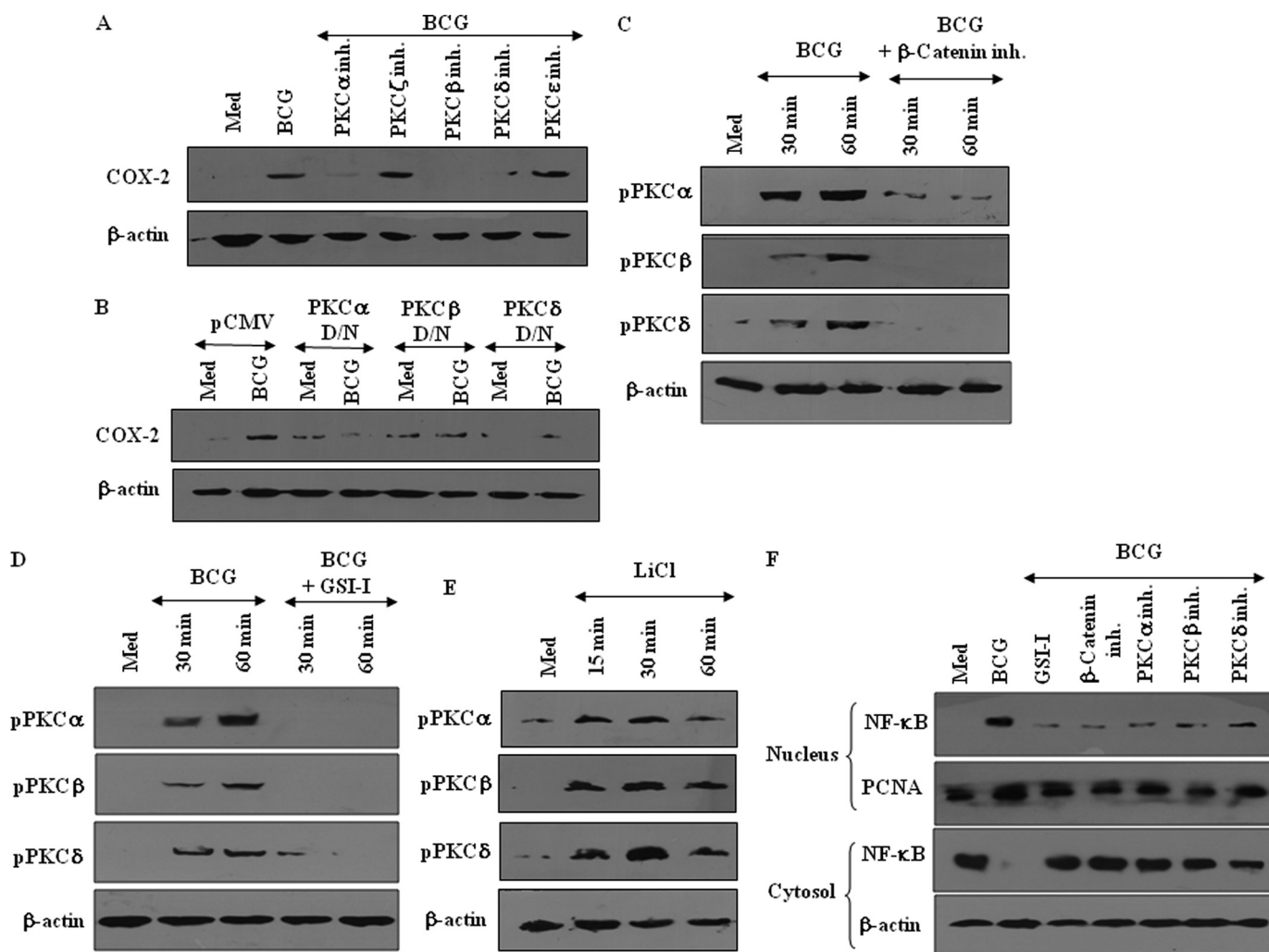
FIGURE 7. **PKC-MAPK-NF-κB signaling orchestrates Wnt-Notch1 axis-mediated pathogenic TLR2 responses.** *A* and *B*, inhibition of PKCα, PKCβ, or PKCδ either by specific pharmacological inhibitors (*A*) or dominant negative (*D/N*) cDNA constructs (*B*) abolishes *M. bovis* BCG-triggered expression of Notch1 target gene COX-2. *C* and *D*, β-catenin inhibitor-mediated inhibition of β-catenin (*C*) or GSI-I-mediated inhibition of Notch1 activity (*D*) compromised the ability of *M. bovis* BCG to trigger activation of PKCα, PKCβ, and PKCδ. *E*, stabilization of β-catenin by LiCl induces activation of PKCα, PKCβ, and PKCδ. *F*, nuclear localization of p65 NF-κB in *M. bovis* BCG-infected macrophages, with or without pretreatment with GSI-I or β-catenin inhibitor or PKCα inhibitor or PKCβ inhibitor or PKCδ inhibitor. The blots are representative of two independent experiments. *Med*, medium.

file of the cells (33, 34). In addition, recent reports advocate strong correlation between Notch and PKC activity in important regulatory functions within various immune cells (35). Furthermore, the steady expansion of innate immune responses initiated by innate immune receptors often involves regulatory action of PKC that acts upstream of activation of MAPK (36, 37). In this perspective, we assessed whether PKC-MAPK and Wnt-Notch1 signaling axis collaborated functionally to regulate the defined set of effector functions in macrophages. As an example, *M. bovis* BCG-triggered expression of Notch1 target gene COX-2 was significantly reduced by pharmacological inhibition of PKC (supplemental Fig. S4A). Furthermore, among specific PKC isoforms, inhibition of PKCα, PKCβ, and PKCδ activity by specific pharmacological inhibitors or dominant negative constructs markedly abolished *M. bovis* BCG-stimulated expression of COX-2 (Fig. 7, *A* and *B*). Accordingly, *M. bovis* BCG challenge led to significant activation of specific PKC isoforms in comparison with *M. smegmatis* and *E. coli*, which could be blocked by pharmacological inhibition of

β-catenin by β-catenin inhibitor or Notch1 by GSI-I (supplemental Fig. S4, *B and C*, and Fig. 7, *C* and *D*). Furthermore, inhibition of GSK-3β by LiCl induced robust activation of specific PKC isoforms (Fig. 7*E*). We had earlier reported that *M. bovis* BCG-triggered expression of Notch1 target gene, COX-2, involves robust activation of Raf1, ERK1/2, and p38 MAPK (16). In this regard, pharmacological inhibition of PKCα, PKCβ, and PKCδ abrogated infection-triggered activation of Raf1, ERK1/2, and p38 MAPK, suggesting PKC-MAPK axis could act as a critical determinant of Wnt-Notch1-mediated cellular responses (supplemental Fig. S4D).

NF-κB is a unique yet a general transcription factor, which in concert with receptor proximal signaling cohorts regulates a range of cellular functions. Interestingly, NF-κB often acts as "gain control" for Wnt-β-catenin- and Notch1-mediated signals (16, 18, 19, 38). In this regard, *M. bovis* BCG infection triggered marked activation of NF-κB as evident by nuclear translocation of the p65 subunit of NF-κB as well as increased binding of nuclear proteins to NF-κB consensus (Fig. 7*F* and
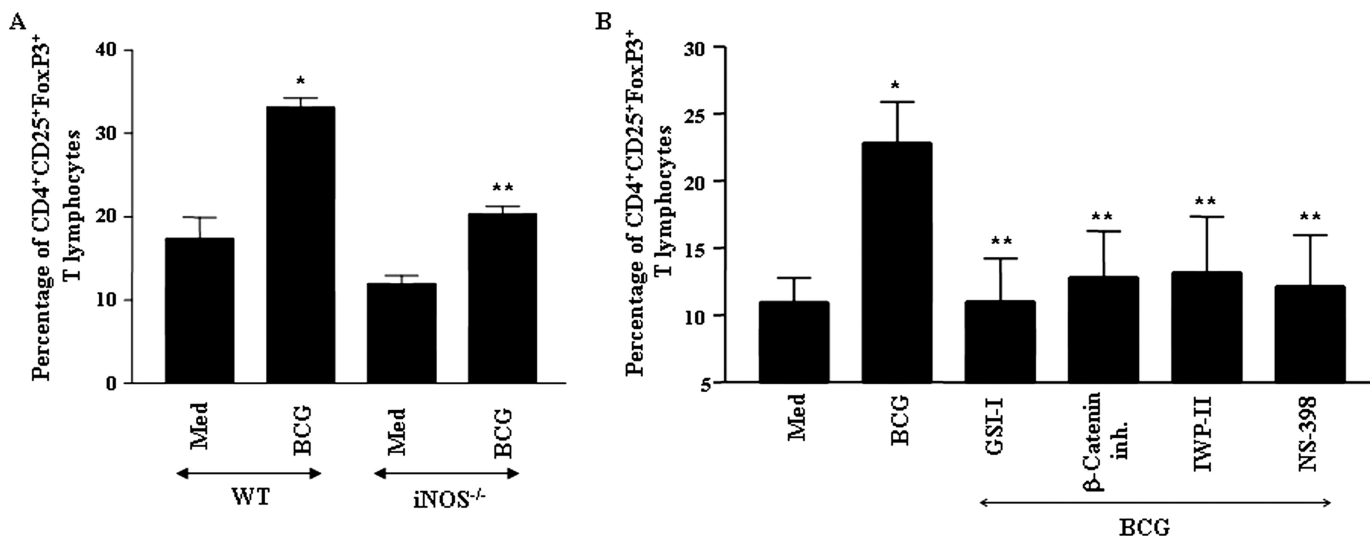
FIGURE 8. **Signaling integration through cross-talk of iNOS, Wnt-β-catenin, and Notch1 signaling controls mycobacterium-specific T$_{Reg}$ cell lineage commitment.** *A*, macrophages derived from *iNOS$^{-/-}$* mice exhibit compromised ability to trigger differentiation of CD4$^+$CD25$^+$FoxP3$^+$ T$_{Reg}$ cells upon infection with *M. bovis* BCG. *B*, inhibition of Notch1 by GSI-I, Wnt-β-catenin by β-catenin inhibitor or IWP-II, and COX-2 by NS-398-impaired *M. bovis* BCG-triggered CD4$^+$CD25$^+$FoxP3$^+$ T$_{Reg}$ cell lineage commitment. *Error bars* represent mean ± S.E. from six independent experiments. *Med*, medium; *WT*, wild type. *, $p < 0.05$ *versus* WT medium; **, $p < 0.05$ *versus* WT BCG.

supplemental Fig. S4*E*). Interestingly, interference in β-catenin, Notch1, or PKC activity reversed *M. bovis* BCG-mediated nuclear translocation of NF-κB from cytosol (Fig. 7*F*). These results suggest that TLR2-activated Wnt-Notch1 and PKC-MAPK signaling axis integrate together to activate NF-κB, which drives activation/expression of the factors involved in regulation of pathogen-specific macrophage functions.

TLR2/iNOS-dependent Activation of Wnt-β-Catenin/Notch1 Signaling Controls T$_{Reg}$ Cell Lineage Commitment—Macrophages tailor immune responses to microbial pathogens by stimulating differentiation of CD4$^+$ T cells into inflammatory or immunoregulatory phenotypes (39–41). Interestingly, recent reports corroborate positive influence of Wnt-β-catenin and Notch1 signaling as well as COX-2 activity in T$_{Reg}$ cell lineage commitment (42–44). It is noteworthy that T$_{Reg}$ cells have been shown to dampen the immune response to a wide range of intracellular pathogens, including mycobacteria (42, 45). In this perspective, we assessed the contribution of pathogen-specific activation of TLR2 signaling in Wnt-β-catenin/Notch1-dependent differentiation of T$_{Reg}$ cells. As shown in Fig. 8, *A* and *B*, priming of splenic T cells with *M. bovis* BCG-infected macrophages resulted in steady increase in percentage of CD4$^+$CD25$^+$FoxP3$^+$ T$_{Reg}$ cells. Interestingly, interference with TLR2/iNOS signaling axis in iNOS null macrophages compromised the ability of *M. bovis* BCG to favor differentiation of T$_{Reg}$ cells (Fig. 8*A*). Importantly, inhibition of β-catenin by the β-catenin inhibitor, secretion of Wnt5a by IWP-II, or activity of Notch1 and COX-2 by GSI-I and NS-398, respectively, led to ablation of *M. bovis* BCG-induced differentiation of T$_{Reg}$ cells (Fig. 8*B*). Together, these results eloquently suggest that pathogen-specific activation of TLR2 signaling exerts cooperative regulation of a distinct set of effector functions in macrophages by virtue of signaling integration involving cross-talk of Wnt-β-catenin and Notch1 signaling.

DISCUSSION

The discriminating responses of innate immunity to invading pathogens often require careful orchestration of signaling events that tailor pathogen-specific defensive measures. This study identifies differential activation of Wnt-β-catenin and Notch1 signaling in response to pathogen-specific activation of TLR2 during infection with *M. bovis* BCG, *S. typhimurium*, and *S. aureus*. Among the tested pathogens, *M. bovis* BCG triggered robust expression of Wnt5a, FzD4, and LRP5, a heightened stabilization and nuclear translocation of β-catenin, thus effectuating the transcriptional activation of Jagged1, and a functional overlap between Wnt-β-catenin and Notch1 signaling.

Bringing correlation with the clinical manifestations of *M. tuberculosis* infection *in vivo*, we could detect augmented expression of signaling cohorts of the Wnt-β-catenin-Notch1 cascade as well as COX-2 and SOCS-3 in peripheral blood mononuclear cells of pulmonary tuberculosis patients or brain samples derived from TBM patients. Induced expression of COX-2 and SOCS-3 acts as a significant factor in influencing the initiation and strength of the mounted innate immune response. The functional attributes of PGE$_2$, product of COX-2 activity, include restrained production of IL-12, IFN-γ, reactive oxygen intermediates, and increased expression of IL-10, thus polarizing skewed acquired immune responses toward immunoregulatory phenotype (46, 47). SOCS-3, a negative regulator of multiple cytokines and Toll-like receptor-induced signaling, is often associated with down-modulation of pro-inflammatory responses during infection with pathogenic microbes (48, 49).

During intensive interplay between signaling pathways, NO serves as a pathological link that modulates direct cooperation of TLR2 with Notch1 signaling to regulate specific components of TLR2 responses (16, 18). Significantly, NO was shown to regulate Wnt-mediated responses in colitis (32). In view of

these observations, we explored whether TLR2-triggered activation of Wnt-β-catenin signaling could fill in the capacity of iNOS/NO to regulate Notch1 responses in iNOS null macrophages. We show that stabilization of β-catenin in $iNOS^{-/-}$ macrophages could trigger the activation of Notch1 signaling as evidenced by activation of γ-secretase complex as well as expression of Notch1 ligand, Jagged1, and Notch1 target gene products COX-2 and SOCS-3.

A series of recent studies have eloquently addressed the relevance of Wnt signaling for lymphocyte development (50, 51). However, information on the role of Wnt signaling in antigen-presenting cells and its impact on differentiation of T cells remains scanty. A seminal study by Manicassamy *et al.* (43) revealed an attractive potential role for Wnt-β-catenin signaling pathway in secretion of immunosuppressive cytokines from dendritic cells, essential for T_{Reg} cell production and generation of tolerance (52). Interestingly, production of T_{Reg} cells, purveyors of immune suppression, is critical for pathogenesis of various intracellular pathogens, including mycobacteria. $CD4^+CD25^+FoxP3^+$ regulatory T cells have been suggested to suppress immunity against *M. tuberculosis* in patients with active disease (42, 45). Furthermore, *in vitro* studies suggest that PGE_2, a biosynthetic product of COX-2 activity, paves a way for the development of T_{Reg} cells (42). In view of these observations, we hypothesized that pathogenic TLR2-activated Wnt-β-catenin signaling could hold the key for T_{Reg} cell lineage commitment. Accordingly, inhibition of Wnt-β-catenin as well as downstream Notch1 signaling and COX-2 activity in macrophages prominently suppressed mycobacterium-induced T_{Reg} differentiation. Furthermore, iNOS null macrophages failed to promote T_{Reg} differentiation upon mycobacterial infection. These results clearly establish that pathogen-specific TLR2 signaling orchestrates differentiation of T_{Reg} cells by virtue of signaling integration through cross-talk of Wnt-β-catenin and Notch1 signaling and induced expression of COX-2.

Overall, the current investigation identifies Wnt-β-catenin as a critical regulator of pathogen-specific TLR2 responses, which in conjunction with Notch1 controls the expression of a battery of genes that could foster the generation of T_{Reg} cells.

REFERENCES

1. Mosser, D. M., and Edwards, J. P. (2008) *Nat. Rev. Immunol.* **8,** 958–969
2. Taylor, P. R., Martinez-Pomares, L., Stacey, M., Lin, H. H., Brown, G. D., and Gordon, S. (2005) *Annu. Rev. Immunol.* **23,** 901–944
3. Pamer, E. G. (2007) *Nat. Immunol.* **8,** 1173–1178
4. Sirard, J. C., Bayardo, M., and Didierlaurent, A. (2006) *Eur. J. Immunol.* **36,** 260–263
5. Albrecht, V., Hofer, T. P., Foxwell, B., Frankenberger, M., and Ziegler-Heitbrock, L. (2008) *BMC Immunol.* **9,** 69
6. Dillon, S., Agrawal, S., Banerjee, K., Letterio, J., Denning, T. L., Oswald-Richter, K., Kasprowicz, D. J., Kellar, K., Pare, J., van Dyke, T., Ziegler, S., Unutmaz, D., and Pulendran, B. (2006) *J. Clin. Invest.* **116,** 916–928
7. Mun, H. S., Aosai, F., Norose, K., Piao, L. X., Fang, H., Akira, S., and Yano, A. (2005) *Infect. Immun.* **73,** 4634–4642
8. Gordon, M. D., and Nusse, R. (2006) *J. Biol. Chem.* **281,** 22429–22433
9. Logan, C. Y., and Nusse, R. (2004) *Annu. Rev. Cell Dev. Biol.* **20,** 781–810
10. Maiese, K., Li, F., Chong, Z. Z., and Shang, Y. C. (2008) *Pharmacol. Ther.* **118,** 58–81
11. Rao, T. P., and Kühl, M. (2010) *Circ. Res.* **106,** 1798–1806
12. Bray, S. J. (2006) *Nat. Rev. Mol. Cell Biol.* **7,** 678–689
13. Collu, G. M., and Brennan, K. (2007) *Breast Cancer Res.* **9,** 105
14. Duncan, A. W., Rattis, F. M., DiMascio, L. N., Congdon, K. L., Pazianos, G., Zhao, C., Yoon, K., Cook, J. M., Willert, K., Gaiano, N., and Reya, T. (2005) *Nat. Immunol.* **6,** 314–322
15. Hayward, P., Kalmar, T., and Arias, A. M. (2008) *Development* **135,** 411–424
16. Bansal, K., Narayana, Y., Patil, S. A., and Balaji, K. N. (2009) *J. Leukocyte Biol.* **85,** 804–816
17. Howe, L. R., Subbaramaiah, K., Chung, W. J., Dannenberg, A. J., and Brown, A. M. (1999) *Cancer Res.* **59,** 1572–1577
18. Kapoor, N., Narayana, Y., Patil, S. A., and Balaji, K. N. (2010) *J. Immunol.* **184,** 3117–3126
19. Narayana, Y., and Balaji, K. N. (2008) *J. Biol. Chem.* **283,** 12501–12511
20. Rodilla, V., Villanueva, A., Obrador-Hevia, A., Robert-Moreno, A., Fernández-Majada, V., Grilli, A., López-Bigas, N., Bellora, N., Albà, M. M., Torres, F., Duñach, M., Sanjuan, X., Gonzalez, S., Gridley, T., Capella, G., Bigas, A., and Espinosa, L. (2009) *Proc. Natl. Acad. Sci. U.S.A.* **106,** 6315–6320
21. Yang, H. Z., Cui, B., Liu, H. Z., Chen, Z. R., Yan, H. M., Hua, F., and Hu, Z. W. (2009) *J. Immunol.* **182,** 692–702
22. Akhtar, S., and Benter, I. F. (2007) *J. Clin. Invest.* **117,** 3623–3632
23. Kircheis, R., Wightman, L., and Wagner, E. (2001) *Adv. Drug Deliv. Rev.* **53,** 341–358
24. Urban-Klein, B., Werth, S., Abuharbeid, S., Czubayko, F., and Aigner, A. (2005) *Gene Ther.* **12,** 461–466
25. Blumenthal, A., Ehlers, S., Lauber, J., Buer, J., Lange, C., Goldmann, T., Heine, H., Brandt, E., and Reiling, N. (2006) *Blood* **108,** 965–973
26. Pereira, C., Schaer, D. J., Bachli, E. B., Kurrer, M. O., and Schoedon, G. (2008) *Arterioscler. Thromb. Vasc. Biol.* **28,** 504–510
27. Mikels, A. J., and Nusse, R. (2006) *PLoS Biol.* **4,** e115
28. Pukrop, T., and Binder, C. (2008) *J. Mol. Med.* **86,** 259–266
29. Rock, R. B., Olin, M., Baker, C. A., Molitor, T. W., and Peterson, P. K. (2008) *Clin. Microbiol. Rev.* **21,** 243–261
30. Beck, K. F., Eberhardt, W., Frank, S., Huwiler, A., Messmer, U. K., Mühl, H., and Pfeilschifter, J. (1999) *J. Exp. Biol.* **202,** 645–653
31. Mannick, J. B., and Schonhoff, C. M. (2002) *Arch. Biochem. Biophys.* **408,** 1–6
32. Wang, H., Zhang, R., Wen, S., McCafferty, D. M., Beck, P. L., and Mac-Naughton, W. K. (2009) *J. Mol. Med.* **87,** 435–445
33. Real, E., Faure, S., Donnadieu, E., and Delon, J. (2007) *J. Immunol.* **179,** 5649–5652
34. Tan, S. L., and Parker, P. J. (2003) *Biochem. J.* **376,** 545–552
35. Jurynczyk, M., Jurewicz, A., Raine, C. S., and Selmaj, K. (2008) *J. Immunol.* **180,** 2634–2640
36. Valledor, A. F., Xaus, J., Comalada, M., Soler, C., and Celada, A. (2000)

J. Immunol. **164,** 29–37

37. Yang, C. S., Lee, J. S., Song, C. H., Hur, G. M., Lee, S. J., Tanaka, S., Akira, S., Paik, T. H., and Jo, E. K. (2007) *Cell. Microbiol.* **9,** 382–396

38. Bournat, J. C., Brown, A. M., and Soler, A. P. (2000) *J. Neurosci. Res.* **61,** 21–32

39. Desmedt, M., Rottiers, P., Dooms, H., Fiers, W., and Grooten, J. (1998) *J. Immunol.* **160,** 5300–5308

40. Gordon, S., and Martinez, F. O. (2010) *Immunity* **32,** 593–604

41. Savage, N. D., de Boer, T., Walburg, K. V., Joosten, S. A., van Meijgaarden, K., Geluk, A., and Ottenhoff, T. H. (2008) *J. Immunol.* **181,** 2220–2226

42. Garg, A., Barnes, P. F., Roy, S., Quiroga, M. F., Wu, S., García, V. E., Krutzik, S. R., Weis, S. E., and Vankayalapati, R. (2008) *Eur. J. Immunol.* **38,** 459–469

43. Manicassamy, S., Reizis, B., Ravindran, R., Nakaya, H., Salazar-Gonzalez, R. M., Wang, Y. C., and Pulendran, B. (2010) *Science* **329,** 849–853

44. Tsukumo, S., and Yasutomo, K. (2004) *J. Immunol.* **173,** 7109–7113

45. Chen, X., Zhou, B., Li, M., Deng, Q., Wu, X., Le, X., Wu, C., Larmonier, N., Zhang, W., Zhang, H., Wang, H., and Katsanis, E. (2007) *Clin. Immunol.* **123,** 50–59

46. Betz, M., and Fox, B. S. (1991) *J. Immunol.* **146,** 108–113

47. Shibata, Y., Henriksen, R. A., Honda, I., Nakamura, R. M., and Myrvik, Q. N. (2005) *J. Leukocyte Biol.* **78,** 1281–1290

48. Croker, B. A., Kiu, H., and Nicholson, S. E. (2008) *Semin. Cell Dev. Biol.* **19,** 414–422

49. Yoshimura, A., Ohishi, H. M., Aki, D., and Hanada, T. (2004) *J. Leukocyte Biol.* **75,** 422–427

50. Staal, F. J., Luis, T. C., and Tiemessen, M. M. (2008) *Nat. Rev. Immunol.* **8,** 581–593

51. van de Wetering, M., de Lau, W., and Clevers, H. (2002) *Cell* **109,** S13–S19

52. Mellman, I., and Clausen, B. E. (2010) *Science* **329,** 767–769
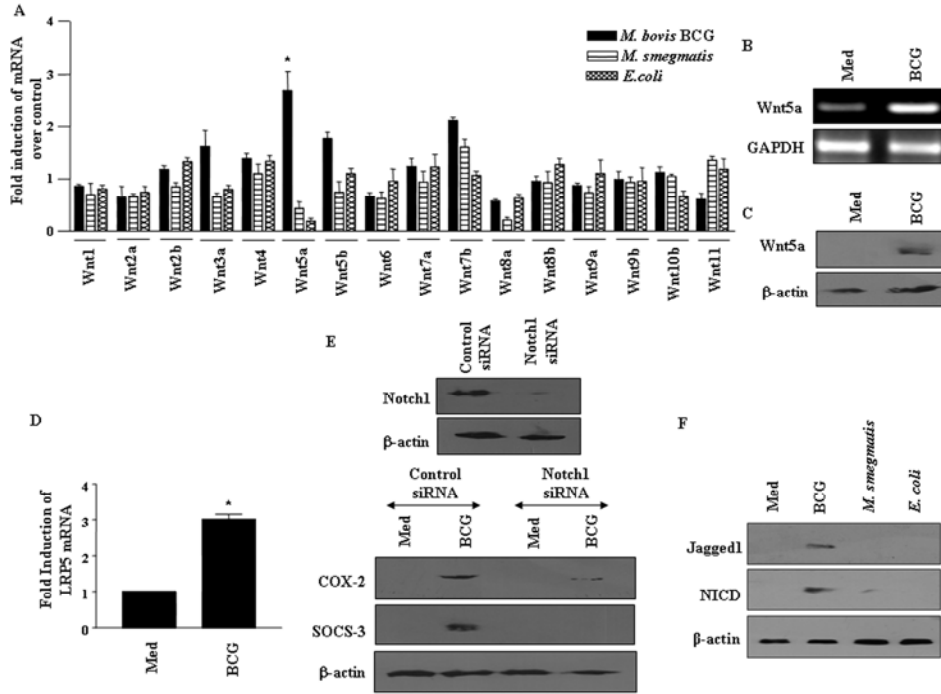
Supplemental FIGURE S1. *Mycobacterium* activates Wnt-β-Catenin and Notch1 Pathway in macrophages. *A*, Expression analysis of Wnt family members in *M. bovis* BCG, *M. smegmatis* or *E. coli* infected macrophages. *B-D*, Infection with *M. bovis* BCG triggers expression of (*B* and *C*) Wnt5a and (*D*) LRP5 as analyzed by (*B*) semi-quantitative PCR, (*C*) immunoblotting and (*D*) quantitative real-time PCR respectively. *E*, siRNA-mediated knock down of Notch1 abrogates *M. bovis* BCG induced expression of COX-2 and SOCS-3. *F*, Compromised ability of *M. smegmatis* and *E. coli* to activate Notch1 signaling in macrophages. The error bars are representing mean ± SE. The data represents three independent experiments. *Med*, Medium. *, $P < 0.05$ *versus* Medium or Control.
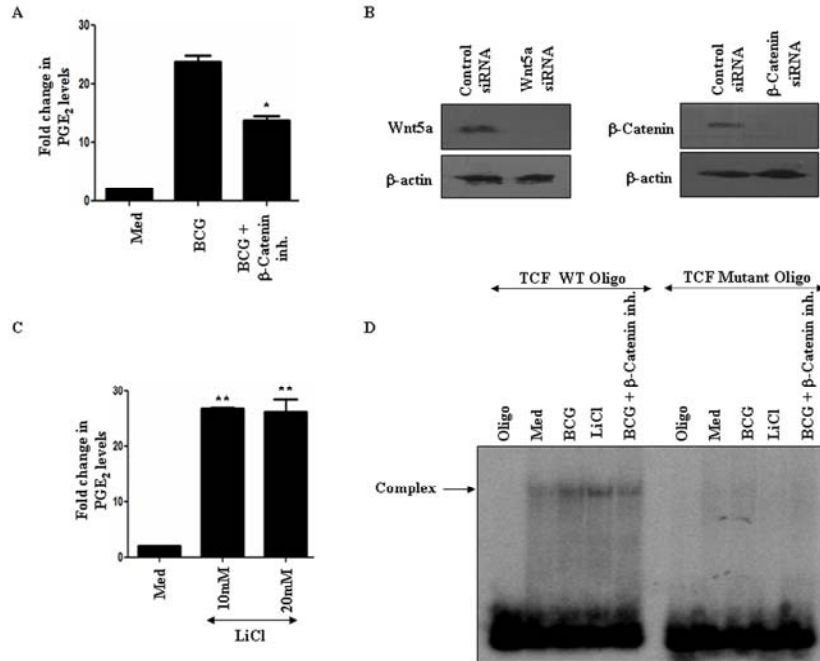
Supplemental FIGURE S2. Wnt-β-Catenin signaling controls activation of Notch1 cascade during mycobacterial infection. *A*, Inhibition of β-Catenin abrogates secretion of PGE$_2$ in *M. bovis* BCG infected macrophages. *B*, siRNA-mediated knock down of Wnt5a and β-Catenin. *C*, LiCl treatment augments PGE$_2$ secretion. *D*, Treatment of macrophages with β-Catenin inhibitor diminishes *M. bovis* BCG triggered binding of TCF at β-Catenin/TCF binding site at mouse Jagged promoter. LiCl promotes binding of TCF at β-Catenin/TCF consensus. The error bars are representing mean ± SE. Data are representative of three independent experiments. *Med*, Medium. *, $P < 0.05$ *versus* BCG; **, $P < 0.05$ *versus* Medium.
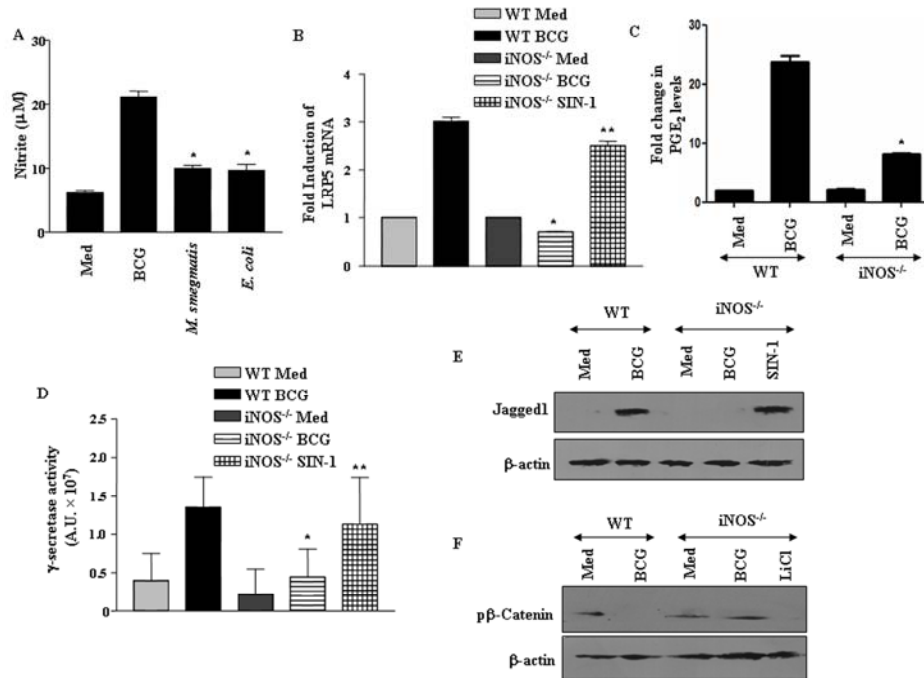
Supplemental FIGURE S3. iNOS/NO is essential for TLR2 mediated regulation of Wnt-β-Catenin signaling. *A*, Infection with *M. bovis* BCG in comparison to *M. smegmatis* or *E. coli* promotes significant increase in NO levels in macrophages. *B*, Expression analysis of LRP5 transcript levels in WT and iNOS$^{-/-}$ macrophages infected with *M. bovis* BCG or iNOS$^{-/-}$ macrophages treated with SIN-1. *C*, Compromised ability of iNOS$^{-/-}$ macrophages to trigger secretion of PGE$_2$ upon infection with *M. bovis* BCG. *D* and *E*, (*D*) Assessment of γ-secretase activity or (*E*) Jagged1 expression in WT macrophages infected with *M. bovis* BCG and iNOS$^{-/-}$ macrophages infected with *M. bovis* BCG or treated with SIN-1. *F*, Phosphorylation status of β-Catenin in WT and iNOS$^{-/-}$ macrophages infected with *M. bovis* BCG or iNOS$^{-/-}$ macrophages treated with LiCl. The error bars are representing mean ± SE. The data are representing three independent experiments. *Med*, Medium; *WT*, Wild type. *, $P < 0.05$ *versus* WT BCG; **, $P < 0.05$ *versus* iNOS$^{-/-}$ BCG.

3
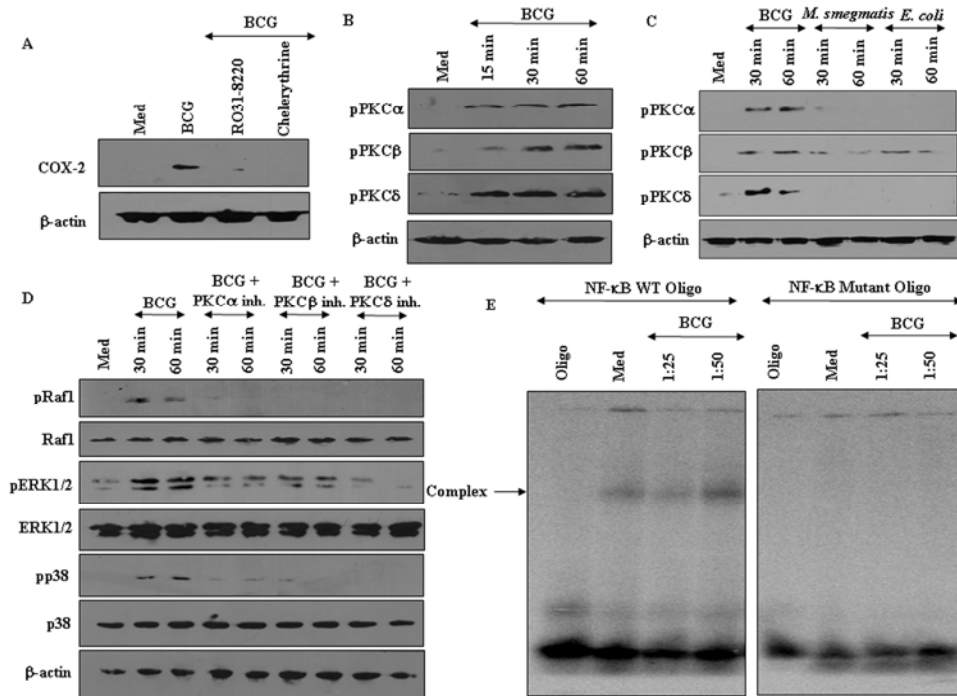
Supplemental FIGURE S4. Essential role for PKC-MAPK-NF-κB axis in execution of pathogen-specific TLR2 responses. *A*, Inhibition of PKC activity by Chelerythrine or RO31-8220 abolishes *M. bovis* BCG triggered COX-2 expression. *B*, Activation of PKCα, PKCβ and PKCδ by *M. bovis* BCG. *C*, Infection with *M. smegmatis* and *E. coli* fails to induce activation of PKCα, PKCβ and PKCδ. *D*, Pharmacological inhibition of PKCα, PKCβ and PKCδ abrogates *M. bovis* BCG induced activation of Raf1, ERK1/2 and p38 MAPK. *E*, *M. bovis* BCG promotes binding of NF-κB to its consensus as analyzed by gel-shift assay. The data represent two independent experiments. *Med*, Medium.

Pathogen-specific TLR2 Protein Activation Programs Macrophages to Induce Wnt- β-Catenin Signaling

Kushagra Bansal, Jamma Trinath, Dipshikha Chakravortty, Shripad A. Patil and
Kithiganahalli Narayanaswamy Balaji

Access the most updated version of this article at doi: 10.1074/jbc.M111.260414

Alerts:
- When this article is cited
- When a correction for this article is posted

Click here to choose from all of JBC's e-mail alerts

Supplemental material:
http://www.jbc.org/content/suppl/2011/08/23/M111.260414.DC1.html

This article cites 52 references, 25 of which can be accessed free at
http://www.jbc.org/content/286/42/37032.full.html#ref-list-1